Optical absorption, excitation, and emission spectra of Eu^{3+} in $LiNbO_3$

L. Arizmendi and J. M. Cabrera
Departamento Optica y Estructura de la Materia, Universidad Autónoma de Madrid, Cantoblanco, 28049 Madrid, Spain
(Received 17 September 1984)

A detailed study of optical absorption, excitation, and emission spectra of Eu^{3+} in the $LiNbO_3$ lattice is presented within the 2700—22 000-cm^{-1} range. The positions of the crystal-field levels in C_3 symmetry are given for the ^7F multiplet and the three lowest levels of the ^5D multiplet. Most of the observed bands are assigned to specific transitions within this scheme, and a simple estimate of the crystal-field parameters is given.

I. INTRODUCTION

$LiNbO_3$ is a ferroelectric crystal having important applications in nonlinear,[1] phase conjugation,[2] and integrated optics[3] devices. Its usefulness in these applications strongly depends on impurity doping and post-growth treatments such as reduction or irradiation.[4–7] Some questions still remain unanswered; e.g., which optical absorption bands correspond to charge-transfer processes, where do impurities locate, or what are the charge-compensation mechanisms? Rare-earth ions have proved to be highly sensitive probes either in optical[8] or EPR (Refs. 9 and 10) spectroscopies to distinguish different crystal-field strengths or symmetries. The structure of their optical spectra is very rich, and the zero-phonon character of their electronic transitions allows wavelength shifts as small as a few angstroms to be clearly detected.

On the other hand, $LiNbO_3$ is a peculiar lattice in which three similar sites are available for cationic impurities, without distorting the main C_3 local symmetry: Li^+, Nb^{5+}, and structural vacancy sites. The sites consist of oxygen octahedral distorted along one of the $\langle 111 \rangle$ axes, which in turn lie on the trigonal ferroelectric axis of the crystal. Since the sizes of the octahedra are about the same in the three cases, the charge of the impurity is expected to play a major role in determining preference among these sites.

Several attempts have been made in the past, without much success, to determine the sites of the Fe^{2+} and Fe^{3+} ions[4,11] in the $LiNbO_3$ lattice, mainly due to their importance in photorefractive damage. From EPR spectra of the Gd:$LiNbO_3$ (Ref. 9) and Nd:$LiNbO_3$ (Ref. 10) systems and from time-resolved spectroscopy[12] and optical absorption measurements[8] of the Eu:$LiNbO_3$ system, two different impurity sites in the $LiNbO_3$ lattice have been found. However, despite these preliminary results, a thorough analysis of the optical spectroscopy of the Eu:$LiNbO_3$ system is still lacking.

In this paper we present, for the first time, a detailed study of the optical absorption, excitation, and emission spectra of the Eu:$LiNbO_3$ system within the (2700—22 000)-cm^{-1} range. Characteristic bands of the Eu^{3+} free ion are observed to be split according to the C_3 local symmetry of the host, much in the same way as has been found in other systems.[13] Most of the observed bands arising from crystal-field interaction are assigned to specific transitions and an estimate of the crystal-field parameters is given.

II. EXPERIMENTAL

Europium-doped $LiNbO_3$ crystals have been pulled in our laboratory from a congruent melt of grade-I Johnson-Mathey powder, under a pure-oxygen atmosphere of 1.1 atm. As a dopant, Eu_2O_3 in concentrations ranging from 0.1 to 3.0 mol % has been added to the melt. Crystals grown in this way look transparent and have a pale, light-rose color. An attempt to grow a 5-mol %-doped crystal resulted in useless polycrystalline boule. From them, (0.5—5.0)-mm-thick plates have been sawed with their faces either parallel or perpendicular to the ferroelectric axis. Optical finishing has been achieved by polishing both faces with 0.3-μm alumina powder as abrasive.

Polarized absorption spectra between 0.300 and 2.5 μm (33 330—4000 cm^{-1}) have been obtained with a Cary 17 spectrophotometer provided with Glan-Thompson—type calcite polarizers. The spectral resolution limit given by the Cary 17 was used, namely, 0.03 nm (between 1.5 and 0.5 cm^{-1}) within the visible range and 1 nm (between 16 and 1.5 cm^{-1}) within the infrared range. To obtain spectra from 2.5 μm (4000 cm^{-1}) to 3.7 μm (2700 cm^{-1}) a fast-Fourier-transform spectrometer (Nicolet DX5) provided with a silver bromide—gold polarizer was used. Within this range this spectrophotometer works with a resolution of 4 cm^{-1}. These specifications were found to be sufficient so that the absorption bands were not distorted, since their bandwidths range from 20 cm^{-1} in the visible region to 100 cm^{-1} in the infrared region. Polarized excitation and unpolarized emission spectra have been obtained with a spectrofluorimeter [Schoeffel Instrument Corp. (N.J.)] provided with a Glan-Thompson—type calcite polarizer after the excitation monochromator exit. Resolution of this equipment was about 1 Å (between 5 and 2 cm^{-1}) within the range of interest) in both excitation and emission monochromators. This also can be considered acceptable in determining the peak positions of the bands. In our setup a polarizer could not be fitted at the emission channel; therefore polarizations of the emission bands have not been determined in this paper. The sam-

ple temperature was changed from 15 K to room temperature by locating it in a closed-cycle helium cryostat, and from room temperature to 450 K by fitting a small furnace within the sample compartment. Diagonalizations of the crystal-field matrices corresponding to the ^7F multiplet were carried out with an IBM 370 VM computer from the IBM-UAM Research Center.

III. EXPERIMENTAL RESULTS

It is well known[14] that the scheme of levels for the free ion Eu^{3+} consists of a ^7F ground-state multiplet well separated from the excited ^5D, ^5G, ^5L, etc., muliplets. $^5D_0$, $^5D_1$, and $^5D_2$ levels are also well separated from any other level, whereas all the remaining levels turn out to be heavily overlapped among them. Either these three ^5D levels or any of the ^7F levels are also sufficiently separated to confirm the assumption that the weak-crystal-field interaction typical of rare-earth ions does not appreciably mix them. In fact, in the recent calculation by Kirby and Richardson[13] for the trigonal C_3 symmetry in the Eu(dibenzoylmethanato)$_3$·H_2O system the maximum admixture found with other levels is 7% for the case of $A(^7F_2)$ level, being smaller for all the other levels mentioned above. This means that assignment of the observed bands can actually be done by labeling the crystal-field levels according to their symmetry, within each J level of the free ion, and applying adequate selection rules.

Within this scheme of levels, the optical absorption and luminescence spectra presented in this paper can be gathered into three groups: (i) absorption spectra in the visible region from the $^7F_0$ level to the $^5D_0$, $^5D_1$, and $^5D_2$ levels, (ii) infrared-absorption spectra from the $^7F_0$ level to the $^7F_4$, $^7F_5$, and $^7F_6$ levels (other transitions within this multiplet fall in the same energy range as the main lattice phonon absorption), and (iii) excitation and emission spectra in the visible region from transitions among all those levels. Since the $^7F_1$ and $^7F_2$ levels are close enough to the $^7F_0$ ground-state level to be thermally populated, absorption and excitation spectra from both levels can be observed at room or higher temperatures. Therefore, low-temperature spectra will help in the achievement of the final assignment, as these transitions will not appear.

As mentioned in Sec. I (see also Ref. 8) we have assumed a C_3 local symmetry for the Eu^{3+} ions, with the threefold axis lying along the ferroelectric axis of $LiNbO_3$. Thus any J level of the free ion will split into a number of A and E crystal-field levels depending on the J value. Since transitions between even J values have electric dipole character and those between odd J values have magnetic dipole character, we must look for both of them. Fortunately, in the $LiNbO_3$ lattice it is possible to experimentally distinguish them by taking the so-called π-, σ-, and α-polarized spectra.

π and σ spectra are taken from samples with the ferroelectric C_3 axis lying along their faces and the electric field of the light beam parallel (for π) and perpendicular (for σ) to the C_3 axis. α spectra are taken from samples with the C_3 axis perpendicular to their faces and the electric field of the light beam perpendicular to the C_3 axis. From these experimental data the character of each transition can be inferred[15] by looking at the selection rules given by group theory. Results are summarized in Table I. In this table z represents the electric dipole along the C_3 axis and (x,y) is the electric dipole perpendicular to C_3 axis; R_z and (R_x,R_y) have similar meanings for the magnetic dipole. In Table II all the observed transitions are shown together with their assignment according to the above rules. As mentioned above, polarizations of the emission bands could not be obtained in our luminescence setup. Let us now comment on specific transitions.

A. $^7F_0$-$^5D_0$ (582.3 nm)

Although this transition (17 173 cm^{-1}) is forbidden, the small admixture with other J levels allows the observation of a small band in absorption, excitation, and emission spectra. It appears for both σ and π polarizations, indicating we are observing magnetic (R_z) and electric (z) dipole transitions. Both of them are allowed by crystal-field interaction as A-A transitions. The optical absorption spectrum shown in Fig. 1 includes this band. It is difficult to say whether this band is split or not, as observed for other bands mentioned below.

B. $^7F_1$-$^5D_0$ (585.8—598.3 nm)

This group of transitions shows absorption and excitation bands at room temperature, where the $^7F_1$ level is thermally populated, and emission bands at room temperature and 15 K. Figure 1 shows the absorption bands observed at room temperature. Two bands can be seen slightly split in this figure: one of them for σ polarization (16 960 cm^{-1}), the other for π and α polarizations (16 736 cm^{-1}). This polarization behavior reflects the magnetic dipole character (see Table I) mentioned before for this transition. The σ band is assigned to the $^7F_1(A)$-$^5D_0(A)$ transition, and the (π,α) band to the $^7F_1(E)$-$^5D_0(A)$ transition. The small splitting of each of these two bands cannot be explained in terms of crystal-field interaction since maximum degeneracy of the $^7F_1$ level is three instead of the four observed peaks. It has been previously explained[8] in terms of the occurrence of two different sites associated with Eu^{3+} ions: one substituting for Nb^{5+}, the other for Li^+.

C. $^7F_2$-$^5D_0$ (617.6—625.4 nm)

This group of transitions contains the strongest emission band observed for Eu^{3+} in $LiNbO_3$. This band (15 990 cm^{-1}) is shown in Fig. 2 together with a second strong one (16 192 cm^{-1}) from this group. They are also observed as very weak excitation bands at room tempera-

TABLE I. Identification of dipole transitions.

Observed polarization	Character
π	z
σ	R_z
π,α	(R_x,R_y)
σ,α	(x,y)

TABLE II. Observed absorption, excitation and emission bands of the Eu^{3+} in the $LiNbO_3$ from 4670 to 36 700 Å.

Wavelength (Å)	Energy (cm^{-1})	Polarization	Absorption coefficient (cm^{-1})	Excitation intensity (u.a.)	Emission intensity (u.a.)	Transition
4670	21 413	σ,α	3.377[a]	3711	58	
			2.229			
4672	21 404	σ,α	3.254[a]	3711	58	$^7F_0(A)-{}^5D_2(E'')$
			2.180			
4675	21 390	π	0.170[a]	339		$^7F_0(A)-{}^5D_2(A)$
			0.080			
4683	21 354	σ,α	4.790[a]	4100	76	
			3.254			
4685	21 345	σ,α	4.780[a]	4100	76	$^7F_0(A)-{}^5D_2(E')$
			3.130			
4711	21 227	σ,α	0.043			
4717	21 220	σ,α	0.104	440	124	$^7F_1(A)-{}^5D_2(E'')$
4722	21 177	σ,α	0.123			
4731	21 137	σ,α	0.092		102	$^7F_1(A)-{}^5D_2(E')$
4736	21 115	σ,α	0.061			
4770	20 964	π		21		$^7F_1(E)-{}^5D_2(E'')$
4775	20 942	σ		42	5	$^7F_1(E)-{}^5D_2(A)$
4888	20 458	σ		39	85	
4894	20 433	π		26	92	$^7F_2-{}^5D_2$
4910	20 367	σ	0.012	72	120	
4955	20 182	σ		18	68	
4985	20 060				30	
5120	19 531	σ		6		
5127	19 505	π		5	42	$^7F_3-{}^5D_2$
5186	19 283	π		10	5	
5279	18 943	π,α	0.233[a]	477	4	
			0.141			
5282	18 932	π,α	0.196[a]	477	10	$^7F_0(A)-{}^5D_1(E)$
			0.123			
5293	18 893	σ	1.167[a]	2060	12	
			0.737			$^7F_0(A)-{}^5D_1(A)$
5296	18 882	σ	1.167[a]	2060	12	
			0.528			
5345	18 709	σ,α	0.025	342	16	$^7F_1(A)-{}^5D_1(E)$
5406	18 498	σ,α	0.380	2415	126	$^7F_1(E)-{}^5D_1(E)$
5413	18 474	σ,α	0.350	2415	126	
5428	18 430				43	$^7F_1(E)-{}^5D_1(A)$
5487	18 225				4	$^7F_4-{}^5D_2$
5544	18 038	σ		9	30	
5574	17 940	π		14	34	$^7F_2(E')-{}^5D_1(E)$
5580	17 921	σ,π		39	31	$^7F_2(E')-{}^5D_1(A)$
5640	17 730	σ,π		3	11	$^7F_2(E'')-{}^5D_1(E)$
5646	17 712	σ		6		$^7F_2(E'')-{}^5D_1(A)$
5684	17 593	σ		15	30	
5724	17 470	σ		6		$^7F_2(A)-{}^5D_1(E)$
5795	17 256	σ		39	23	
5823	17 173	σ,π,α	0.037[a]	66	68	$^7F_0(A)-{}^5D_0(A)$
			0.018			
5858	17 071	σ		57	137	
5895	16 964	σ	0.190	1090	777	$^7F_1(A)-{}^5D_0(A)$
5901	16 946	σ	0.166	1090	731	
5920	16 892				160	$^7F_3-{}^5D_1$
5975	16 736	π,α	0.025	192	1714	$^7F_1(E)-{}^5D_0(A)$
5983	16 714	π,α	0.025	192	1714	
6010	16 639				297	$^7F_3-{}^5D_1$
6176	16 192	σ		20	2515	$^7F_2(E')-{}^5D_0(A)$
6254	15 990	σ		30	8230	$^7F_2(E'')-{}^5D_0(A)$

TABLE II. (*Continued*).

Wavelength (Å)	Energy (cm^{-1})	Polarization	Absorption coefficient (cm^{-1})	Excitation intensity (u.a.)	Emission intensity (u.a.)	Transition
6540	15 291				160	
6553	15 260				320	$^7F_3-{}^5D_0$
6570	15 221				107	
6923	14 445				330	$^7F_4(E)-{}^5D_0(A)$
6946	14 397				375	$^7F_4(A)-{}^5D_0(A)$
7026	14 233				570	$^7F_4(E)-{}^5D_0(A)$
7062	14 160				514	$^7F_4(A)-{}^5D_0(A)$
7068	14 148				715	$^7F_4(E)-{}^5D_0(A)$
7126	14 033				195	$^7F_4(A)-{}^5D_0(A)$
7180	13 928				14	$^7F_6-{}^5D_1$
7505	13 324				81	
7570	13 210				129	$^7F_5-{}^5D_0$
7606	13 147				105	
7670	13 038				12	
18 900	5291	π	1.412[a]			$^7F_0(A)-{}^7F_6(A)$
			1.105			
19 011	5260	π	1.412[a]			$^7F_0(A)-{}^7F_6(A)$
			1.105			
19 260	5192	σ,α	0.123[a]			$^7F_0(A)-{}^7F_6(E)$
			0.184			
19 600	5102	π	0.675[a]			$^7F_0(A)-{}^7F_6(A)$
			0.522			
19 900	5025	π	0.491[a]			$^7F_0(A)-{}^7F_6(A)$
			0.460			
19 952	5012	σ,α	5.649[a]			$^7F_0(A)-{}^7F_6(E)$
			4.973			
20 239	4941	σ,α	4.544[a]			$^7F_0(A)-{}^7F_6(E)$
			3.807			
20 899	4785	π	0.829[a]			$^7F_0(A)-{}^7F_6(A)$
			0.982			
20 942	4775	σ,α	0.890[a]			$^7F_0(A)-{}^7F_6(E)$
			1.289			
21 552	4640	σ,α	0.061			$^7F_1-{}^7F_6$
22 002	4545	σ,α	0.614			
25 445	3930	σ,α	0.491			
26 247	3818		0.184			
27 701	3610		0.307			$^7F_0-{}^7F_5$
29 851	3350		0.061			
31 847	3140	π	0.614			$^7F_0(A)-{}^7F_4(A)$
33 058	3025	σ,α	0.685			$^7F_0(A)-{}^7F_4(E)$
33 113	3020	π	1.903			$^7F_0(A)-{}^7F_4(A)$
34 048	2937	σ,α	1.781			$^7F_0(A)-{}^7F_4(E)$
36 101	2770	π	0.978			$^7F_0(A)-{}^7F_4(A)$
36 697	2725	σ,α	0.921			$^7F_0(A)-{}^7F_4(E)$

[a]Data taken at 15 K.

ture for σ and α polarizations (see Table II). This fact allows the assignment to electric dipole transitions between the two E levels coming from crystal-field splitting of the $^7F_2$ level and the $^5D_0(A)$ level. No band has been observed that could be assigned to the $^7F_2(A)$-$^5D_0(A)$ transition.

D. ($^7F_3$,$^7F_4$,$^7F_5$)-$^5D_0$ (654.0—767.9 nm)

Weak emission bands have been observed for these groups of transitions. Their intensity is very low even in the crystals with the highest Eu concentration (3%). Only the group coming from $^5D_0$-$^7F_4$ exhibits sufficient intensi-

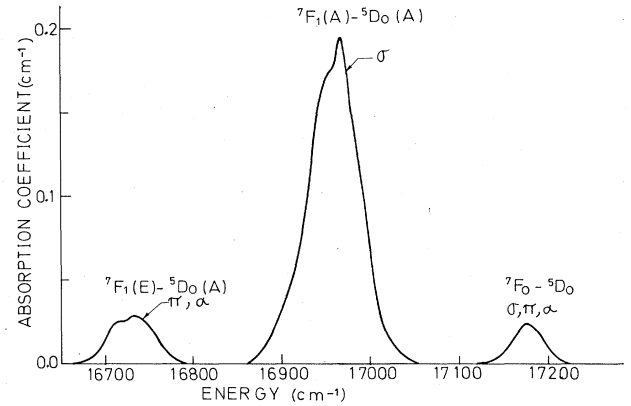

FIG. 1. Optical absorption bands arising from $(^7F_0, ^7F_1)$-$^5D_0$ transitions in the $LiNbO_3$—(3 mol %) Eu^{3+} system at room temperature.

ty and separation to be studied [Fig. 3(a)]. Although their polarization could not be determined from our emission setup, comparison with the absorption bands from the $^7F_0$-$^7F_4$ group, discussed below, allows the assignment to be done (see also Fig. 4). From the weak emission spectra observed for $^7F_3$-$^5D_0$ and $^7F_5$-$^5D_0$ groups nothing can be said except they are there (see Table II).

E. $^7F_0$-($^7F_4$,$^7F_5$,$^7F_6$) (1.890—3.670 μm)

These groups of transitions have been observed by infrared optical absorption. The bands observed for the $^7F_0$-$^7F_4$ group [Fig. 3(b)], together with the emission bands from the $^5D_0$-$^7F_4$ group commented on above, have permitted a safe location of the $3A+3E$ crystal-field levels arising from the $^7F_4$ level. Therefore the $^7F_4$ splitting is adequate for use in the crystal-field parameter estimate, to be discussed in Sec. IV. From the $^7F_0$-$^7F_6$ group, some intense absorption bands have also been observed, although they exhibit a strong overlap. Since we could not observe the $^5D_0$-$^7F_6$ emissions with our emission setup, it is difficult to locate the $^7F_6$ crystal-field levels. Even less can be drawn from the few heavily overlapped absorption

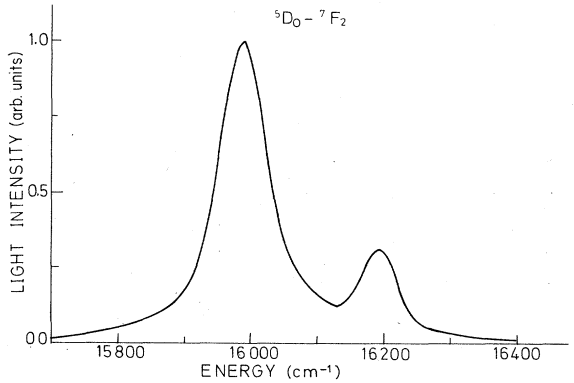

FIG. 2. Emission bands associated to $^5D_0$-$^7F_2$ transitions in the $LiNbO_3$—(3 mol %) Eu^{3+} system at room temperature. Excitation at the $^7F_0(A)$-$^5D_2(E')$ transition (21 354 cm^{-1}).

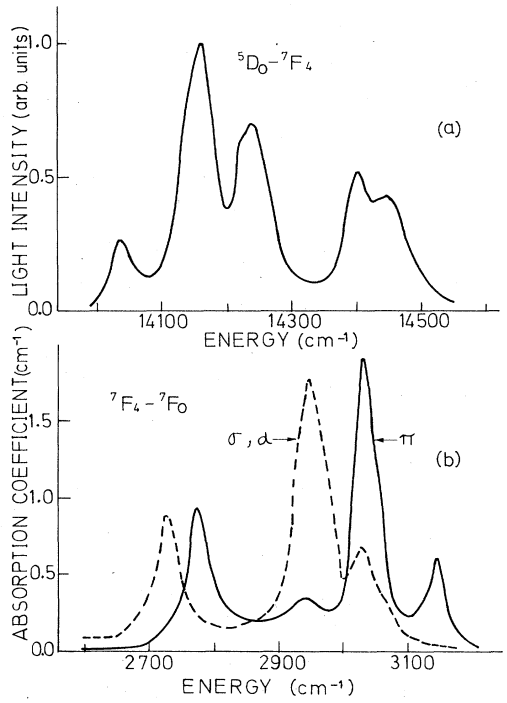

FIG. 3. (a) Emission bands associated to $^5D_0$-$^7F_4$ transition in the $LiNbO_3$—(3 mol %) Eu^{3+} system at room temperature, exciting at 21 354 cm^{-1}. (b) Infrared absorption bands arising from $^7F_0$-$^7F_4$ transitions.

bands of the $^7F_0$-$^7F_5$ group. On the other hand, as mentioned above, no transitions between $^7F_0$ and $(^7F_1, ^7F_2, ^7F_3)$ levels can be observed since their energies fall into the main phonon absorption of the $LiNbO_3$ lattice.

F. $(^7F_0, ^7F_1)$-$(^5D_1, ^5D_2)$ (467.0—542.6 nm)

Strong absorption and excitation as well as weak emission spectra were observed for these groups of transitions. The two $^7F_0(A)$-$^5D_1(A,E)$ magnetic dipole (Fig. 5) and the two $^7F_0(A)$-$^5D_2(E,E')$ electric dipole (Fig. 6) transi-

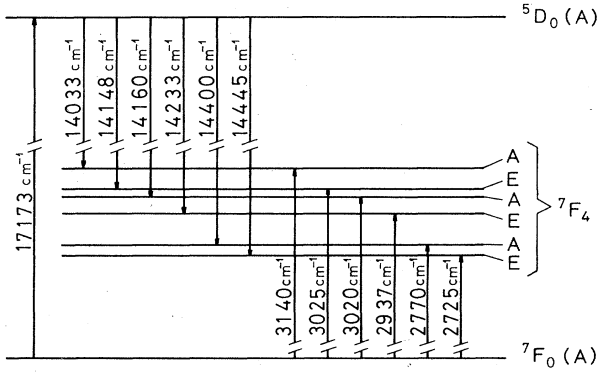

FIG. 4. Location of the crystal-field levels arising from the $^7F_4$ free ion level. The undegenerated $^7F_0$ ground and $^5D_0$ levels are taken as reference (compare with Table II and Fig. 3).

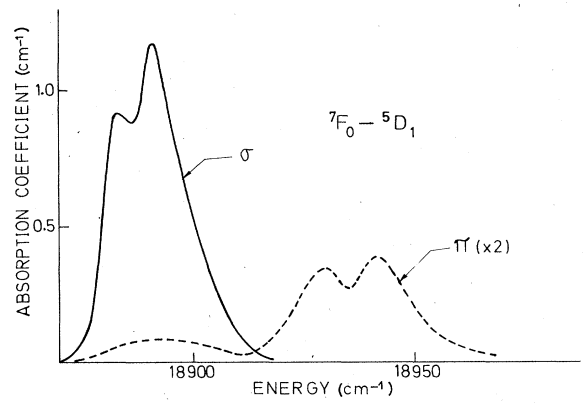

FIG. 5. Optical absorption bands originated from $^7F_0$-$^5D_1$ transitions in the $LiNbO_3$—(3 mol %) Eu^{3+} system at 15 K mainly magnetic dipole character.

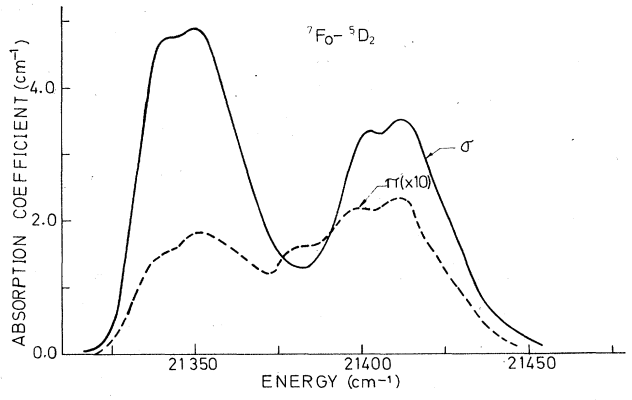

FIG. 6. Optical absorption bands arising from $^7F_0$-$^5D_2$ electric dipole transition in the $LiNbO_3$—(3 mol %) Eu^{3+} system at 15 K.

tions appear to be split into a greater number of bands than expected from crystal-field interaction. As mentioned before for the $^7F_1$-$^5D_0$ group these splittings have been attributed[8] to the occurrence of two different sites for Eu^{3+} ions: Li^+ and Nb^{5+} sites. The assignment of these bands makes it possible to locate the $^5D_1$ and $^5D_2$ crystal-field levels, as well as to further support the previous location of the $^7F_1(A,E)$ levels.

Other small bands observed in absorption, excitation, and emission spectra (see Table II) were used to check the self-consistency of the band assignment and level location. From transitions to and from the $^7F_0$ ground level (shown in Table II) the final scheme of crystal-field levels for the ^7F multiplet, and $^5D_0$, $^5D_1$, and $^5D_2$ levels can be easily obtained. Individual labeling for those corresponding to the $^7F_3$, $^7F_5$, and $^7F_6$ levels cannot be safely given from our experimental data.

IV. DISCUSSION

Results presented in Sec. III, particularly the assignments made in Table II for the observed absorption, excitation, and emission bands, strongly support the assumed C_3 symmetry for the Eu^{3+} ion in the $LiNbO_3$ lattice. These results are also in agreement with the assumption made in Refs. 8 and 16 where C_{3v} symmetry, previously used by other workers to fit optical spectra, was disregarded for Eu^{3+} and Ni^{2+} ions, respectively. From the polarization behavior it is inferred that the threefold local axis lies along the trigonal axis of the lattice. Therefore local charge-compensation defects, if any, must lie along the ferroelectric axis. As mentioned before three sites are available for cations in the $LiNbO_3$ lattice showing C_3 local symmetry: Li^+ and Nb^{5+} sites plus a structural vacancy. In a previous paper[8] some evidence that Eu^{3+} ac-

TABLE III. Experimental and calculated crystal-field splittings of the $^7F_0$,$^7F_1$,$^7F_2$ of the Eu^{3+} free-ion levels. (1) and (2) refer to the two lattice sites commented on in the text.

J	Level	Experimental energy (cm^{-1})	Calculated energy (cm^{-1})	E_c (cm^{-1})
0	A	0	0	0
1	A	209 (1)	209 (1)	375.7 (1)
		227 (2)	227 (2)	367 (2)
	E	437 (2)	437 (2)	
		459 (1)	459 (1)	
2	E	981	981	
	A		995.5 (1)	1064.7 (1)
			1022.7 (2)	1070.1 (2)
	E	1183	1183	
4	E	2725	2725	2922.1
	A	2770	2770.2	
	E	2937	2937.8	
	A	3020	3019.4	
	E	3025	3022.4	
	A	3140	3139.5	

TABLE IV. Crystal-field parameters in cm^{-1}.

Parameter	B_{20}	B_{40}	B_{60}	B_{43}	B_{63}	B_{66}
Site 1	−350	−34	−30.9	±2414	±77	1036
Site 2	−417	−23.8	−33	±2198	±84	1074

tually substitutes for both cations Li^+ and Nb^{5+} was reported. By growing Eu-doped $LiNbO_3$ crystals with different [Li]/[Nb] ratios, we tried to selectively populate either the Li^+ or Nb^{5+} sites. All the split bands whose two peaks were attributed to two different sites were observed to change the relative height of their peaks. The fact that the absolute value of the charge balance, as well as the ionic radius are the same for both sites, further supports the assumption that the Eu^{3+} is, in fact, located in both sites with similar probability. Moreover, time-resolved spectroscopy measurements[12] have shown a probability of finding two Eu^{3+} ions in neighboring positions higher than a random distribution. These two positions could be Li^+ and Nb^{5+} adjacent sites. In any case most of the Eu^{3+} ions seem to be scattered throughout the lattice, and a long-range charge-compensation mechanism is likely to be operating as well. This kind of charge-compensation mechanism is commonly found in the $LiNbO_3$ lattice.[1]

Also to be noted is the relatively large bandwidth observed in all the Eu^{3+} spectra. This feature is often found in optical and EPR spectra[1] of most dopants in $LiNbO_3$ and has been previously explained in terms of the large strains present in this lattice. Under these strains the crystal field shows a large continuous range of values.

A simple estimate of the crystal-field parameters has been carried out by using the observed splittings of the ^7F multiplet levels. Only the experimentally well-established levels, i.e., $^7F_0, ^7F_1, ^7F_2, ^7F_4$, have been used in the fitting process. To do this we have disregarded matrix elements mixing different ^7F_J levels; thus we are dealing with well-separated ^7F_J matrices which can be independently diagonalized. This assumption is not unreasonable since the mixing elements between the closest levels ($^7F_0$ and $^7F_1$) are zero and the rest are well separated among them. In fact, a more detailed recent calculation for the trigonal (C_3 symmetry) Eu(dibenzoylmethanato)$_3$·H_2O system[13] has shown that maximum admixture for the levels we are using in the fitting is less than 5%.

For the estimate of the crystal-field parameters the occurrence of two sites associated with Eu^{3+} has been taken into account via the $^7F_1$ level. It has been possible due to the fact that the two crystal-field levels arising from the $^7F_1$ level show site splitting, and their positions are experimentally well determined. Therefore, for each site, one parameter set has been obtained.

The splitting of each of the ^7F levels can be expressed in terms of the crystal-field contribution to the Hamiltonian. This crystal-field Hamiltonian is most conveniently written in the operator-equivalent form. For the trigonal symmetry this Hamiltonian is

$$H_J = \alpha_J B_{20} O_{20} + \beta_J B_{40} O_{40} + \gamma_J B_{60} O_{60} + \beta_J B_{43} O_{43} + \gamma_J B_{63} O_{63} + \gamma_J B_{66} O_{66} ,$$

where B_{nm} are the familiar "optical parameters," O_{nm} are operator-equivalent expressions, and α_J, β_J, and γ_J are the operator-equivalent factors.[17] The various entries in the matrices, $\langle JM \mid H_J \mid JM' \rangle$, are readily evaluated from published tables.

In the fitting process a number of diagonalizations and subsequent comparisons of the eigenvalues with the experimental data have been performed. The well-defined splittings of the $^7F_1$ level directly gives a first estimate of B_{20}. The remaining parameters were slowly varied until a good fitting was achieved. Table III shows both calculated and experimental splittings for the sets of parameters giving the best fitting. The values of these parameters are shown in Table IV.

ACKNOWLEDGMENTS

We wish to thank Professor F. Agulló-López for useful discussions and criticism of the manuscript. Thanks are also given to Mr. F. Abella for technical assistance in the crystal growth of the $LiNbO_3$ crystals. Work partially supported by Comisión Asesora de Investigación Científica y Técnica (CAICyT).

[1] A. Raüber, in *Current Topics in Materials Science,* edited by E. Kaldis (North Holland, Amsterdam, 1978), Vol. 1, pp. 481–601. (This is a general convenient review on $LiNbO_3$.)

[2] P. Günter, Phys. Rep. **93**, 199 (1982).

[3] H. F. Taylor, Ferroelectrics **50**, 141 (1983).

[4] M. G. Clark, F. J. DiSalvo, A. M. Glass, and G. E. Peterson, J. Chem. Phys. **59**, 6209 (1973).

[5] R. J. Holmes, V. S. Kim, C. D. Brandle, and D. M. Smith, Ferroelectrics **51**, 41 (1983).

[6] J. L. Ketchum, K. L. Sweeney, L. E. Halliburton, and A. F. Armington, Phys. Lett. A **94**, 450 (1983).

[7] L Arizmendi, J. M. Cabrera, and F. Agulló-López, J. Phys. C **17**, 515 (1984).

[8] L. Arizmendi, F. Abella, and J. M. Cabrera, Ferroelectrics **56**, 75 (1984).

[9] B. Dischler, J. R. Herington, A. Rauber, J. Schneider, and W. Urban, Solid State Commun. **12**, 737 (1973).

[10] G. Burns, D. F. O'Kane, and R. S. Title, Phys. Rev. **167**, 314 (1968).

[11] V. N. Belogurov, V. A. Bylinkin, I. V. Gotlib, N. M. Rubinina, and P. E. Sen'kov, Fiz. Tverd. Tela (Leningrad) **18**, 143 (1976) [Sov. Phys.—Solid State **18**, 80 (1976)]; Y. V. Vladi-

mirtsev, V. A. Golenishchev-Kutuzov, S. A. Migachev, and N. A. Shamukov, Ferroelectrics **22**, 653 (1978).

[12]J. K. Tyminski, C. K. Lawson, and R. C. Powell, J. Chem. Phys. **77**, 4318 (1982). See also C. K. Lawson, Ph.D. thesis, Oklahoma State University, 1981.

[13]A.F. Kirby and F. S. Richardson, J. Phys. Chem. **87**, 2544 (1983).

[14]G. S. Ofelt, J. Chem. Phys. **38**, 2171 (1963).

[15]See, for example, P. P. Feofilov, *The Physical Basis of Polarized Emission* (Consultants Bureau, New York, 1961), English translation of *Polyarizovannaya Lyuminestsentsiya Atomov, Molekul i Kristallov* (State Physica—Mathematical Press, Moscow, 1959).

[16]L. Arizmendi, J. M. Cabrera, and F. Agulló-López, Ferroelectrics **56**, 79 (1984).

[17]B. R. Judd, Mol. Phys. **2**, 407 (1959).